Transient biogeochemistry in intertidal sediments: New insights from tidal pools in Zostera noltei meadows of Arcachon Bay (France)

Sylvain Rigaud, B. Deflandre, O. Maire, G. Bernard, J.C. Duchêne, D. Poirier, P. Anschutz

Accepted Manuscript

Transient biogeochemistry in intertidal sediments: New insights from tidal pools in Zostera noltei meadows of Arcachon Bay (France)

S. Rigaud, B. Deflandre, O. Maire, G. Bernard, J.C. Duchêne, D. Poirier, P. Anschutz

This is a PDF file of an unedited manuscript that has been accepted for publication. As a service to our customers we are providing this early version of the manuscript. The manuscript will undergo copyediting, typesetting, and review of the resulting proof before it is published in its final form. Please note that during the production process errors may be discovered which could affect the content, and all legal disclaimers that apply to the journal pertain.

Transient biogeochemistry in intertidal sediments: new insights from tidal pools in *Zostera noltei* meadows of Arcachon Bay (France)

S. Rigaud[1,2,*], B. Deflandre[1], O. Maire[1], G. Bernard[1], J.C. Duchêne[1], D. Poirier[1], P. Anschutz[1]

[1]EPOC, UMR CNRS 5805, University of Bordeaux, Pessac, France

[2]Univ. Nîmes, EA 7352 CHROME, rue du Dr Georges Salan, 30021 Nîmes, France

[*]Corresponding author: sylvain.rigaud@unimes.fr. Present address: Univ. Nîmes, EA 7352 CHROME, rue du Dr Georges Salan, 30021 Nîmes, France.

Abstract

Several studies highlighted the occurrence of circular pools in intertidal flats of different coastal systems and their transient water chemistry over both tidal and diurnal cycles. However, little is known about (1) the response of benthic biogeochemical reactions and fluxes at the sediment-water interface over such short time scales, and (2) the role of these tidal pools in the biogeochemical functioning of coastal systems. Based on *in situ* microprofiles and water sampling, we investigated the dynamics of dissolved oxygen (O_2), nutrients, sulfides and metals, and the associated fluxes at the sediment-water interface in tidal pools from the Arcachon Bay (Atlantic coast of France). Our integrative approach included several tidal and diurnal cycles over two different seasons in the presence and absence of *Zostera noltei*. The results show that water temperature and light irradiance were the main factors driving the biogeochemical functioning of the tidal pools, as they controlled the physiological activity of the microphytobenthos. Changes in light radiations induced diurnal fluctuations of O_2 concentrations within surficial sediment, thus resulting in fluctuations of the O_2 diffusive fluxes at the sediment-water interface and of the O_2 penetration depth in sediment. At high tide, the increase in turbulence above the sediment induced the advection of oxygenated water within the first millimeters of sediment, resulting in a significant increase in porewater O_2 concentrations and sediment O_2 penetration depth. Porewater sulfide concentrations and apparition depth were concomitant with the O_2 dynamic over both diurnal and tidal cycles, indicating that intermediate redox diagenetic processes were impacted by O_2 dynamic over such short time-scale. The rapid changes in redox processes in the sediment column are confirmed by a significant flux of dissolved manganese toward the water column during nighttime. The consumption of nitrate and the release of ammonium and phosphate, associated to the mineralization of the organic matter in the surface sediment did not appeared related however to such short time cycles. The efflux of dissolved silica from the sediment was most likely associated with the enhanced dissolution of Si-bearing particles in surface sediment at higher temperatures, although silica uptake by *Z. noltei* was also noted. This study clearly shows that tidal pools function as natural incubators of transient biogeochemical processes. A rough assessment of the nutrient budget at the scale of the bay indicates the tidal pools may contribute significantly to the biogeochemical functioning of Arcachon Bay.

Keywords: tidal pools; biogeochemistry; sediment-water interface; fluxes; *Zostera noltei*

1. Introduction

In shallow coastal areas, the functioning of pelagic and benthic compartments is tightly coupled (Soetaert et al., 2000). Physical and chemical properties, such as temperature light, salinity, concentration of dissolved oxygen and nutrients, strongly vary over time scales ranging from hours to years in the coastal water column due to tidal, diurnal and seasonal cycles. These environmental evolutions profoundly impact the sediment biogeochemistry and chemical exchanges at the sediment-water interface, which in turn impact the water column chemistry. Assessing the transient dynamics of sedimentary biogeochemical processes is of primary importance to better understand the functioning of coastal ecosystems and to predict their evolution in a changing world.

Intertidal zones are particularly suitable to investigate the transient dynamics of sedimentary biogeochemical processes as they undergo strong changes in light, temperature, nutrient availability and hydrodynamic conditions over time, from tidal to seasonal time scales (e.g., Taillefert et al., 2007; Jansen et al., 2009). Recent works showed that the intensity of light irradiance was the main factor controlling the short-term O_2 dynamic in intertidal sediments over diurnal and tidal cycles (Jansen et al., 2009; Denis et al., 2012; Delgard et al. 2012). During the daytime, O_2 generally presents higher concentrations and penetration depths in sediments due to the photosynthetic activity of microphytobenthos, which may result in a net O_2 production in surface sediments and O_2 flux from the sediment to the water column (Bottcher et al., 2000; De Beer et al., 2005; Werner et al., 2006; Jansen et al., 2009; Delgard et al., 2012). Moreover, Denis et al. (2012) indicated that benthic photosynthetic production was generally higher during emersion periods than during inundation periods, as the light irradiance could be strongly attenuated through the water column. Previous studies also reported a vertical migration of microphytobenthos during tidal cycles in intertidal sediments that significantly modified the photosynthetic activity in surficial sediments (Consalvey et al., 2004; Migné et al., 2009; Denis et al., 2012; Delgard et al. 2012). The changes in O_2 concentration in surficial sediments directly impact the fate of redox species through modifications of early diagenetic processes such as denitrification, nitrification, and metal (e.g., Fe and Mn) and sulfide oxidation (Deflandre et al., 2002; Dalsgaard, 2003; Taillefert et al., 2007; Glud, 2008; Rigaud et al., 2013). Indeed, the increase in O_2

penetration depth in sediments lowers the sulfate reduction rates (Billerbeck et al., 2006) and intensifies the oxidation of reduced species produced in the anoxic part of the sediment (NH_4^+, Fe^{2+}, sulfides S(-II) and FeS; Taillefert et al., 2007; Delgard et al., 2012), thereby directly modifying the exchanges of nutrients and metals at the sediment-water interface (Rigaud et al., 2013).

The main limitation in understanding the biogeochemical processes and chemical transfers at the sediment-water interface in intertidal environments is the specific conditions occurring at low tide, notably the emersion periods that interrupt the exchanges at the sediment-water interface and induce perturbations such as the evaporation of porewater and desiccation of the top layer of sediments. Interestingly, intertidal flats may present topographic depressions where water can be trapped during low tide (e.g., Van der Laan and Wolff, 2006). These environments, referred as tidal pools, are particularly exposed to temporal variations in light and temperature because of their small volumes and shallow depths (e.g., Morris and Taylor, 1983; Clavier et al., 2011). Tidal pools have transient chemical compositions over tidal cycles due to chemical exchanges at the sediment-water interface (Lillebø et al., 2004; Murray et al., 2006). Thus, tidal pools can be considered as natural incubators, where it is possible to investigate the dynamics of sedimentary biogeochemical processes in response to changes in the environmental conditions in the overlying water. Indeed, the benthic-pelagic coupling is expected to be amplified due to the reduced volume of the pelagic compartment.

In the present study, we characterized the transient biogeochemistry of sediments in response to the variation of external forcing (temperature, light, water depth) over tidal and diurnal cycles in tidal pools from the Arcachon Bay. Biogeochemical processes and fluxes at the sediment-water interface were characterized and quantified from continuous *in situ* measurement of O_2, H_2S and pH in porewaters using an autonomous miniprofiler and from temporal variations of major biogeochemical species concentration (O_2, NO_3^-, tCO_2, PO_4^{3-}, NH_4^+, Si_d, Mn_d and Fe_d) in the overlying water trapped in the pool at low tide. The contribution of driving factors was evaluated by statistical treatments. A chemical budget at the scale of the bay is proposed to estimate the role of tidal pools to the biogeochemical functioning of Arcachon Bay.

2. Material and Methods

2.1. Study area and sampling

The tidal pools were located in an intertidal mudflat of Arcachon Bay (44°42.737N; 1°08.097W), a macrotidal lagoon along the French Atlantic coast characterized by a semi-diurnal tide with an amplitude ranging from 1.2 m to 4.4 m (Figure 1A). The pools at the study site were topographic depressions, a few meters wide and up to 20 cm depth (Figure 1B). Lagoon water was trapped in the pools for approximately 4-5 hours around low tide, until the rising tide reached the study site. The intertidal flat consisted of silty loam sediment colonized by a dense meadow of the dwarf eelgrass *Zostera noltei*. Although their origin is still not known (i.e., hydrodynamic vs. biological structure; see discussion in Van der Laan and Wolff, 2006; Takeuchi and Tamaki, 2014), the tidal pools presented consistent features in Arcachon Bay. Aerial photos of the sampling site enabled to estimate a surface coverage of 20% for the tidal pools (Figure 1C). Arcachon lagoon pools were similar to those previously described by van der Laan and Wolff (2006) in the Banc d'Arguin (Mauritania).

Three field campaigns were carried out in July 2010 and August and October 2013. In July 2010, four different pools were studied during the same day: two pools densely covered by *Zostera* noltei and two unvegetated pools (Table 1). The water trapped in the four pools was sampled in triplicate every hour throughout an emersion period in the daytime (between 13:30 and 16:20). Pools studied in August and October 2013 were both unvegetated. In August 2013, the pool water was sampled during two consecutive periods of emersion, including one daytime (between 14:40 and 18:40) and one night (between 02:20 and 06:30). In October 2013, the pool water was sampled during emersion periods occurring during three consecutive days (between 12:00 and 18:00). Both in August and October 2013, sampling of the pool water started approximately one hour before the complete disconnection of the pool during the ebb tide and finished about one hour after the pools reconnected with the bay water during the flood tide. Water samples were collected in the central part of the pool using a 250 mL Nalgene beaker fixed on a long rod with a sampling frequency of 20-30 minutes. Samples were immediately filtered using acetate cellulose 0.2 µm syringe filters and were partitioned in either plastic or glass vials according to the type of analysis to be performed. The subsamples were stored untreated in gastight glass vials for total dissolved inorganic carbon ($tCO_2 = CO_2 + HCO_3^- + CO_3^{2-}$) analysis or

collected in polyethylene vials and acidified with a 1% equivalent volume of concentrated HNO_3 for dissolved Fe and Mn analysis. The subsamples for dissolved nutrients (NO_3^-, NH_4^+, PO_4^{3-}, Si_d) analysis were transferred into two 12 mL polyethylene vials. Samples for tCO_2, metals and Si_d were kept refrigerated until analysis, while those for other nutrients were immediately frozen. The analysis of these samples was completed within a month after sampling.

At the end of 2013 campaigns, three 10 cm long and 2.5 cm diameter sediment cores were collected and sliced at 2 mm vertical resolution for porosity assessment. Porosity was obtained on each sediment slice by mass differences between fresh and freeze-dried sediment following correction for salt content, and assuming a sediment particle density of 2.65 $g.cm^{-3}$.

2.2. *In situ* measurements in the pool water

Temperature, salinity, dissolved O_2 concentration, photosynthetically active radiation (PAR) reaching the sediment surface and water pressure (i.e., depth) were continuously monitored in the pools using *in situ* autonomous probes. Oxygen concentration and temperature were recorded using a SDOT300 data logger (*NKE Instruments*) equipped with an *Aanderaa* optode 3835. Salinity, temperature and water pressure were recorded using a STPS 100-SI data logger (*NKE Instruments*). PAR was monitored using a SPAR data logger (*NKE Instruments*) equipped with a flat LI-192 sensor (*LI-COR Corporate*). The SDOT and STPS probes were mounted on a foot of the miniprofiler MP6 system (see below) and positioned to be immerged in the pool water, while the SPAR probe was directly inserted into the pool sediment. During the 2010 campaign, the SDOT and STPS sensors were deployed in only one of the four pools, while temperature was manually recorded in the other at each sampling time. Oxygen concentrations were compensated for salinity, temperature and depth using the Interactive TD 280 spreadsheet (AADI, *Aanderaa*). The precisions of measurements were ± 5% for oxygen, 0.1°C for temperature, 0.1 for salinity and 0.1 m for water depth. Water depth within the pools was precisely measured in the field with a ruler. All parameters were recorded every 5 minutes.

2.3. *In situ* microelectrode measurements

The vertical distribution and temporal evolution of temperature, pH, O_2 and H_2S at the sediment-water

interface were measured using an autonomous *in situ* miniprofiler MP6 system (*Unisense A/S*). The miniprofiler was deployed at high tide during the two campaigns of 2013, but only the data obtained during the October campaign was exploitable. The benthic MP6 miniprofiler is a 6-channel system equipped with a temperature sensor (200 μm tip), a pH sensor (500 μm tip) with a reference electrode, a H_2S sensor (100 μm tip) and three oxygen sensors (100 μm tips). The tips of the temperature, H_2S and pH sensors were positioned at the same level, which was 25 mm below the oxygen sensors tips, and manually positioned on field at about 10 mm above the sediment-water interface. The reference electrode was mounted on the frame of the profiler to be continuously emerged. Two sets of measurements were carried out sequentially. The first set consisted of measurements along vertical profiles from +10 mm to -45 mm (temperature, pH, and H_2S sensors) and from +35 mm to -20 mm (oxygen sensors) across the sediment-water interface. The vertical resolution was 1 mm for the upper 25 mm, and 0.1 mm below. Once the profiles were completed (i.e., approximately 100 minutes), the sensors returned to their initial position, moved horizontally by approximately 1 cm and were put on hold for 30 minutes before starting the next profiling sequence. The profiling experiment lasted approximately 48 hours, providing 29 depth profiles of temperature, pH and H_2S and 87 depth profiles of O_2. Then, the sensors were introduced into the sediment for a time-series recording for 24 hours. The three oxygen sensors were precisely (± 0.1 mm) located at 0.5, 1.1 and 1.7 mm depth below the sediment-water interface, while the temperature, H_2S and pH sensors were at 25 ± 1 mm below the interface. Measurements were carried out every 5 seconds. The pH sensor was calibrated just before deployment at the *in situ* temperature with reference NBS standards (*Metrohm Ltd.*) and corrected from the *in situ* temperature shift during deployment. The H_2S sensor was calibrated in the laboratory before and after each deployment using a N_2 bubbled pH4 buffer solution in which successive volumes of a precisely titrated Na_2S stock solution were added. Oxygen sensors were calibrated using the *in situ* O_2 concentration in the pool water measured with an *Aanderaa* optode and the zero O_2 concentration of the anoxic sediment.

2.4. Laboratory analyses

Water samples were analyzed for NO_3^- (Hansen and Koroleff, 2007), NH_4^+ (Koroleff, 1976), PO_4^{3-}

(Murphy and Riley, 1962) and Si_d (Truesdale and Smith, 1976) using a Quattro-AXFLOW autoanalyzer. Concentration of dissolved Mn was determined by flame atomic absorption spectrometry (AAnalyst 300, Perkin Elmer). Concentration of dissolved Fe was determined by spectrophotometry (Stookey, 1970). tCO_2 was analyzed by flow injection analysis (FIA) as described by Hall and Aller (1992). The limits of quantification associated with these techniques are 0.2 µM for nutrients, 0.2 µM for Mn_d, and 0.5 µM for Fe. The relative uncertainties estimated from replicates were better than 5%.

2.5. Computation of benthic exchanges in tidal pools

Benthic exchanges in the tidal pools were obtained using two methods. The diffusive oxygen flux at the sediment-water interface (J_{dif}) was first calculated from the oxygen concentration gradient measured with microelectrodes during the profiling experiment. Oxygen profiles were treated, and diffusive fluxes were calculated with a modified version of the PRO_2FLUX program software (Deflandre and Duchêne, 2010) using Fick's law:

$$J_{dif} = -\phi D_s \frac{\delta O_2}{\delta z} \qquad (1)$$

where ϕ is the porosity, D_s is the oxygen molecular diffusion coefficient corrected for sediment temperature and tortuosity (Boudreau, 1997), and $\frac{\delta O_2}{\delta z}$ is the measured oxygen concentration gradient at the sediment-water interface.

In the second approach, flux calculation was based on temporal changes in the concentrations of chemical species in the pool water. Total fluxes at the sediment-water interface (J_T in $\mu mol.m^{-2}.h^{-1}$) were calculated from the slope of the linear concentration change over time ($\propto$ in $\mu mol.m^{-3}.h^{-1}$) and the water depth (h in m) in the pool water according to:

$$J_T = \propto h \qquad (2)$$

This allowed the estimation of the total flux during the period of complete disconnection of the pool from the bay water. Field observations showed that for approximately one hour after the pool water was disconnected from the bay water, water still flowed through the pool from the surrounding tidal

flat and from upstream connected tidal pools. Consequently, the pool was a closed system only when this flow ceased. Total flux calculation was thus only applied for this specific period of time. Pelagic processes that can induce chemical changes in the water column are integrated in this approach. However, given the relatively low height of water column (i.e., <12 cm), the effect of pelagic processes on the chemical composition of the pool water are expected to be negligible in comparison to the effect of benthic exchanges. Atmospheric deposition was not considered here, as no rain events occurred during the field campaigns. In addition, the influence of evaporation was shown to be negligible (see discussion below). Fluxes of O_2 and tCO_2 at the sediment-water interface could not be assessed as exchanges at the pool water-atmosphere interface may occur.

2.6. Statistical treatments

The significance level of slopes used for flux calculations in the pool water was tested. Only slopes that significantly differed from 0 (t-test, $p<0.05$) were considered as indicative of existing fluxes. In addition, the differences in each pair of slopes leading to fluxes calculation for a given chemical species were tested using slope homogeneity tests (after concentration data was standardized by the pool water height). The obtained p-values were therefore corrected for multiple comparison using the Holm-Bonferonni method. Two slopes with corrected p-value <0.05 were thus considered as significantly different.

The contributions of environmental factors explaining the temporal variability in (1) the pool water O_2 and tCO_2 concentrations in each investigated pool during disconnection from the bay water, (2) processes at the water-sediment interface (diffusive O_2 fluxes, O_2 penetration depth and H_2S appearance depth) in the pool continuously monitored for two days in October 2013, and (3) sediment chemistry (dissolved O_2 and H_2S concentrations and pH in the sediment) in the pool continuously monitored for 24 hours in October 2013, were investigated using a distance-based redundancy analysis (dbRDA) performed with the DistLM option in PERMANOVA + add-on for PRIMER (Anderson et al., 2008). Forward selection was used to build models using AIC selection criterion. Pool water O_2 and tCO_2 concentrations and O_2 concentrations at 0.5, 1.1 and 1.7 mm depth in the sediment were respectively used as response multivariate data cloud defined using Euclidean distance amongst

samples. Oxygen diffusive fluxes and penetration depth, H_2S appearance depth in the sediment and pH and H_2S concentration at 2.5 cm depth in the sediment were used separately as single response variable. Tested predictor variables included pool water temperature, PAR, water depth and sediment temperature at 2.5 cm depth in the sediment.

3. Results

3.1. Biogeochemical dynamics in the overlying water of the tidal pool

The biogeochemical composition of the water trapped in the pools at low tide exhibited strong temporal changes (Figures 2 and 3). Water temperature fluctuated by >10°C amplitude over tidal and diurnal cycles, ranging between 41°C in July 2010 during the day and 12°C in October 2013 during nightime (Figure 2). The salinity remained constant (32.5 ± 0.3) when the pools were connected to the bay water. After disconnection, the salinity increased over time by up to 3.4 and 1.0 units during daytime in July 2010 and in 2013, respectively, while the salinity was steady (± 0.2 unit) during the night. During the July 2010 campaign, when conditions for evaporation were optimum, the salinity increased by 11%. Not surprisingly, the PAR reaching the sediment surface in the pool was higher when the pool was disconnected from the bay water (i.e., when the water depth was the lowest). Oxygen concentration was relatively constant around 190-220 μM (i.e., 80-95% air saturation) when the pools were connected to the bay waters (Figure 2). Once disconnected during daytime and when the water from the intertidal flat ran off through the pool, O_2 concentration strongly increased up to 250-480 μM (i.e., 120-210% air saturation). After the run-off stopped, O_2 concentration slightly decreased over time. Conversely, O_2 content decreased down to 35-50% air saturation (i.e., 80-150 μM) during the night. The concentration of tCO_2 showed the opposite trend, with a strong decrease during daytime and an increase during the night while being relatively constant when pools were connected to the bay waters (Figure 3).

Dissolved inorganic nitrogen and phosphate remained at low concentrations in pool waters: $\leq$5 μM for NO_3^-, $\leq$6 μM for NH_4^+ and $\leq$0.6 μM for PO_4^{3-} (Figure 3). NO_3^- and NH_4^+ concentrations were even below the quantification limit in July 2010. The PO_4^{3-} concentration increased over time in the pool water during the disconnection periods. NO_3^- concentration decreased when the pools were

disconnected from the bay waters, while the concentration of NH_4^+ increased with a more scattered evolution and the presence of peaks. The concentration of Si_d always decreased when the water of the intertidal flat ran off through the pools and then steadily increased with time until the bay water re-inundated the pools (Figure 3). Dissolved Mn content in pool water remained low during the daytime. During the night, a marked and regular increase in Mn_d was observed in August 2013. Dissolved Fe was always below the quantification limit (<0.5 μM; data not shown).

3.2. Biogeochemical dynamic in the tidal pool sediment

The vertical and temporal changes in pH, temperature, and O_2 and H_2S concentrations in pool sediments measured in October 2013 are presented in Figures 4 and 5. Temperature exhibited strong fluctuations in the upper 5 cm of sediment concomitant with temperature changes in the overlying water, although the amplitude of thermal shift decreased with sediment depth. As an example, temperature varied between 16 and 24°C at the interface, while it varied between 18 and 22°C at 4 cm depth (Figure 4).

When the pool was connected to the bay water, O_2 concentration decreased from 80-200 μM in the overlying water to 0 μM at 1.7±0.3 mm (Figure 4). During daytime, when the pool was disconnected from the bay water, the O_2 concentration increased in the surficial sediment to values up to 600 μM, resulting in a significant increase in O_2 penetration depth up to 2.6 ± 0.4 mm. Similar trends were observed at the beginning of the time-series experiment during daytime with O_2 concentrations of ~500 μM at 0.5 mm depth and ~450 μM at 1.1 mm depth (Figure 5). Deeper at 1.7 mm depth, the O_2 concentration fluctuated between 0 and 150 μM. During the night, O_2 concentration decreased to values <150 μM at 0.5 mm depth and close to 0 μM deeper. Surficial sediment O_2 concentration increased after the re-connection between the pool and the bay waters during both daytime and night flood tides (Figure 5).

The apparition depth of H_2S (Z_{H2S}), which refers here to a concentration ≥ 1 μM, varied between -5 and -20 mm (Figure 4). The maximum concentration measured at -4.5 cm fluctuated between 25 and 175 μM. The minimum Z_{H2S} and the highest H_2S concentrations were observed during the night, and the maximum Z_{H2S} and lower H_2S concentrations occurred during the daytime. In addition, H_2S

concentration at -25 mm depth was significantly lower at high tide when the pool was connected to the bay water (Figure 5).

In pool water, pH reached 9.7 during daytime, 8.0 during the night, and was intermediate at high tide (Figure 4). The pH decreased in surface sediment, with minimum values at depths between -5 and -10 mm depth. A minimum pH value of 7.3 was measured in this layer when the pool was disconnected during the night. Deeper, pH values were between 7.6 and 8.2. The pH was approximately 8.15 during the 24-h monitoring at -25 mm depth (Figure 5).

3.3. Chemical exchanges at the sediment-water interface

Diffusive O_2 flux (J_{O2}) at the sediment-water interface exhibited strong fluctuations over time (Figure 4). J_{O2} was from the overlying water to the sediment, and relatively constant when the pool was connected to the bay water (-375 ± 100 $\mu mol.m^{-2}.h^{-1}$). J_{O2} slightly decreased (-230 ± 70 $\mu mol.m^{-2}.h^{-1}$) when the pool was disconnected from the bay water during the night. During daytime disconnection, J_{O2} was directed from the sediment to the overlying water, reaching up to 1290 $\mu mol.m^{-2}.h^{-1}$.

When significant, the flux of NO_3^- calculated from the evolution of concentration in the pool waters over time, was always negative while the fluxes of NH_4^+, PO_4^{3-}, Si_d and Mn_d were always positive (Table 1). The calculated fluxes of NO_3^-, NH_4^+ and PO_4^{3-} did not exhibit significant differences between conditions. Fluxes of Si_d were significantly different between daytime and night conditions and between seasons (Table 1). The flux of Si_d in unvegetated pools exhibited a positive correlation with the average temperature in the pool water (Figure 6). For similar temperature conditions in July 2010, the flux of Si_d in vegetated pools (339-426 $\mu mol.m^{-2}.h^{-1}$) appeared lower than in unvegetated pools (605-620 $\mu mol.m^{-2}.h^{-1}$). A high flux of Mn_d was obtained during night conditions in August, whereas the flux was one order of magnitude lower during daytime conditions in both August and October 2013.

4. Discussion

Several studies have shown the occurrence of circular pools in intertidal flats of different coastal systems (e.g., Smith and Able, 1994; Van der Laan and Wolff, 2006; Takeuchi and Tamaki, 2014,

Wilson et al., 2014). However, little is known about the role of tidal pools in the biogeochemical dynamic of coastal sediments (Jensen and Muller-Parker, 1994) because reports on the diagenetic evolution of redox species in tidal pool sediments are scarce (Lillebø et al., 2004; Murray et al., 2006). The dataset obtained from the tidal pools in the *Zostera sp.* meadows of Arcachon Bay gives a unique opportunity to better understand the biogeochemical dynamics of these small-scale ecosystems and their potential impact at a larger scale. In the following discussion, we present the environmental factors that control the transient biogeochemistry of these tidal pools. Then, we show how tidal pools may help to better understand the biogeochemical functioning of coastal ecosystems, and their potential contribution to the water quality of Arcachon Bay.

4.1. Dynamics of physicochemical conditions in the tidal pool water

Temperature and light irradiance greatly changed in the pools over the course of the study (Figure 2). Changes in temperature in the pool water over tidal and diurnal cycles reached an amplitude of up to 10°C, similar to the variations reported in tidal rock pools by Morris and Taylor (1983). Although with a lower amplitude, temperature changes also occurred in surface sediment. In contrast, salinity in the pools remained constant (± 0.5 unit) when connected to the bay water and slightly increased in the pools during periods of disconnection. The maximum increase in salinity was observed during the daytime, likely as a consequence of the evaporation of pool water. Assuming that the salt or water exchanges were negligible between the water pools and the sediment or surrounding area during pool complete isolation, the relative volume of water evaporated from the pools was ≤ 3% for the daytime and ≤ 1% for the night in August and October 2013 and ≤ 11% in July 2010, which suggests that the consequence of evaporation on biogeochemical processes can be neglected.

4.2. Transient biogeochemistry of O_2 and tCO_2

Changes in temperature and light irradiance in aquatic ecosystems primarily impact the photosynthetic and respiration activity of organisms, and hence the dynamic of O_2 and tCO_2. As expected, we observed opposite fluctuations of O_2 and tCO_2 concentrations at diurnal scale (Figures 2 and 3). The dynamics of O_2 and tCO_2 appeared strongly governed by both light and temperature, as between 75.0

and 94.7% of the variance in O_2 and tCO_2 concentration are explained by PAR and temperature (Table A1). The photosynthetic activity in the pool is mainly attributed to the activity of microphytobenthos. Indeed, the highest O_2 concentrations were always recorded in the uppermost sediment layer during the daytime (Figures 4 and 5). The O_2 production in surface sediment induced O_2 fluxes from the sediment to the water column (Figure 4), which is in agreement with previous field studies (de Beer et al., 2005; Jansen et al., 2009; Denis et al., 2012; Delgard et al., 2012). The control of benthic photosynthetic activity on the O_2 dynamic in the pool water is supported by the fact that changes in PAR and temperature significantly accounted together for 72.5 % of the temporal variation of the oxygen concentrations in the surface sediment during the time-series experiment and changes in PAR alone for 80.7 % of the temporal variations of the O_2 diffusive fluxes at the sediment-water interface during the profiling experiment (Table A2). During nighttime, the decrease in O_2 concentration in the pool water (Figure 2) may be attributed to the respiration of the benthic fauna living in the pool and O_2 consumption by the sediment for microbial respiration and oxidation reactions. Benthic O_2 uptake estimated by the diffusive transport of O_2 at the sediment-water interface was -230 ± 70 $\mu mol.m^{-2}.h^{-1}$ (n=16) during the night in October 2013. Assuming that this flux was homogeneous over the pool surface, the resulting decrease in water column O_2 concentration (ΔO_2) due to diffusive benthic uptake is given by the following expression:

$$\Delta O_2 = \frac{JO_2 \cdot t}{h}$$

where t is the time of pool isolation (4 h), J_{O_2} is the mean O_2 diffusive flux, and h is the water height (12 cm). The calculated ΔO_2 value is 7.7 ± 2.4 μM, which is 2-10 times lower than the effective decrease in O_2 measured during the night (i.e., 15-70 μM). This suggests that O_2 uptake in the pool water was mostly due to fauna activity, in agreement with *ex situ* core incubations previously carried out in the same area (Delgard et al., 2013; Delgard et al., 2016a).

In the pool sediment, the O_2 concentration was shown to be transient with variations of several tens of μM within minutes in relation to both diurnal and tidal cycles. Two major processes may be involved in the changes in O_2 concentrations and penetration depths in pool sediments. The first one is

associated with the variations in the activity of microphytobenthos in surface sediment over diurnal and tidal cycles as previously described. The production of O_2 in surface sediment during the daytime when pools were disconnected from the bay water allowed a deeper O_2 diffusion into the sediment. This process is supported by the high proportion (63.4%) of the temporal variation of O_2 penetration depth in sediment that could be explained by changes in temperature and PAR together during the profiling experiment (Table A2). The second process involved in the observed changes in O_2 in the pool sediments is associated with tides. Indeed, O_2 concentrations increased in the surface sediment when the pool became connected to the bay water (Figure 5). The water depth during immersion also contributed significantly in explaining changes in O_2 concentration in surface sediment during the time-series experiment (Table A2). This coupling may be due to porewater circulation induced by waves and currents during the increasing height of the water column at rising tide (De Beer et al., 2005; Billerbeck et al., 2006; Werner et al., 2006; Jansen et al., 2009; Delgard et al., 2012), causing a higher hydrostatic pressure, which drives porewater movements through the sediments (Precht et al. 2004). This phenomenon is well known to have a significant impact in permeable sediments (Huettel and Webster 2001; Charbonnier et al., 2016) but is limited in cohesive sediments. Although hydrodynamics is quite reduced in intensity in this area of Arcachon Bay (Ganthy et al. 2013), our results indicate that advective flushing may act upon benthic biogeochemistry at a millimeter scale. Such observation could not have been possible *in situ* outside a tidal pool. The cumulated effect of PAR, temperature and water level are thus able to explain 74.0% of the total variance of oxygen concentration in surface sediment in the studied tidal pool (Table A2).

4.3. Transient diagenetic processes in the tidal pool

The sulfide profiles measured in October 2013 revealed that the H_2S concentrations in sediment porewaters also exhibited strong vertical and temporal dynamics (Figure 4). Dissolved sulfide production resulted from bacterial sulfate reduction coupled to organic carbon oxidation when other oxidants (i.e., O_2, NO_3^-, Mn and Fe oxides) are depleted (Jørgensen, 1982). These fluctuations were in phase with the O_2 concentration variations: the lowest H_2S apparition depth and the highest H_2S concentration generally corresponded to the lowest oxygen concentrations (i.e., during the night when

the pools were isolated). In addition, the water depth could significantly explain 78.7% of the temporal variation of H_2S concentrations at -2.5 cm during the time-series experiment (Figure 5, Table A2). This indicates that the O_2 production and the flushing of oxygenated water in surface sediment were an efficient forcing controlling the dynamic of porewater H_2S concentrations. However, we always noticed a significant gap of 9 ± 4 mm between the O_2 penetration depth and the H_2S apparition depth in sediment (Figure 4). This suggests that O_2 was not the primary oxidant of H_2S. It is worth noting that a rapid and direct H_2S oxidation by O_2 through cable bacteria may be involved here, as reported by Nielsen and Risgaard-Petersen (2015) and Malkin and Meysman (2015), although we could not prove that this process was occurring in the studied tidal pools. Intermediate redox processes with a rapid kinetic (within minutes time-scales) involving nitrogen, manganese or iron species may possibly act as electron transfers between O_2 and H_2S within this depth interval of a few millimeters. Interestingly, our results show that the Mn_d concentration increased in the pool water during isolation from the bay water (Figure 3), with corresponding effluxes one order of magnitude higher during nightime than during daytime (Table 1). The buildup of dissolved Mn in the pool water can be directly associated with the release of Mn from sediments due to the reductive dissolution of Mn-oxyhydroxides below the thin oxic layer of the sediment. The oxic layer is enriched in Mn oxides, acting as a diffusion barrier for the dissolved Mn (Kristiansen et al., 2002; Pakhamova et al., 2007; Rigaud et al., 2013). As the oxic layer became thinner during night, porewater Mn_d was produced closer to the surface sediment, facilitating its release to the pool water. This indicates that redox processes involving at least Mn species may act as an intermediate redox processes for electron transfer between O_2 and H_2S over diurnal timescales. The absence of measurable content of Fe in the pool waters indicates that most of the Fe diffusing up from deeper sediments was re-oxidized within the oxic layer, preventing its release and accumulation in the pool water (Sundby et al., 1986; Kristiansen et al., 2002; Pakhamova et al., 2007; Rigaud et al., 2013).

The uptake of NO_3^- and release of NH_4^+ and PO_4^{3-} indicate that denitrification and OM (i.e., organic P and N) mineralization processes controlled the dynamic of those nutrients at the sediment-water

interface of tidal pools. However, no clear trend was identified over the diurnal and tidal cycles, suggesting that these ongoing redox processes occurred over longer time scale.

The Si_d fluxes in unvegetated pools was shown to be positively related with average temperature (Figure 6). This may be partly attributed to the increase in molecular diffusivity of Si_d with temperature. However, the Si_d diffusion coefficient increases by 45% between 20 and 35°C (Boudreau, 1997), whereas we observed an increase in Si_d flux by more than 600%. As the quartz solubility is between 122 and 240 µM of H_4SiO_4 and between 1475 and 2380 µM for amorphous silica in the range of temperature measured in pools (Gunnarsson and Arnorsson, 2000), Si_d in pool waters was far below equilibrium with respect to quartz and biogenic silica. This suggests that the Si_d release in the tidal pools was likely related to the dissolution of Si-bearing particles or biogenic silica debris in surface sediment, its accumulation in porewaters and diffusion to the water column, all processes being further enhanced under higher temperature (Feuillet-Girard et al., 1997). In vegetated pools, the release of Si_d appeared lower than in unvegetated pools (Table 1) suggesting Si_d uptake by *Zostera noltei*. Although aquatic macrophytes contain significant amounts of biogenic silica (Schoelynck et al., 2010), only a few works have reported on the Si uptake by marine macrophytes (Herman et al., 1996; Glé et al., 2008; Querné et al., 2012).

4.4. Importance of the tidal pools ecosystems in the biogeochemical functioning of Arcachon Bay

Environmental conditions prevailing in the tidal pools induced the release and accumulation of PO_4^{3-}, NH_4^+, Si_d and Mn_d during the period of isolation. Then, tidal pool waters mix with the lagoon waters at rising tide contributing to the input of chemical species into the bay. The intertidal flats of the bay have a surface area of 115 km^2 (Plus et al., 2009). The surface area of tidal pools represents 17 km^2, assuming that pools cover 20% of the intertidal flats. Considering the range of fluxes measured in the unvegetated tidal pools (Table 1) and an average emersion period of 6 h at each tidal cycle, we calculated net fluxes up to 450 kmol.y^{-1} for PO_4^{3-}, 12000 kmol.y^{-1} for NH_4^+, 62000 kmol.y^{-1} for Si_d and 4000 kmol.y^{-1} for Mn_d. Phosphate inputs from tidal pools are of the same magnitude as the dissolved

inorganic phosphorus supplied by the continental waters that flow to the Arcachon Lagoon (Buquet et al., 2017). The flux of ammonium from tidal pools corresponds up to 18% of the average annual inputs of dissolved inorganic nitrogen from the drainage basin (Canton et al. 2012), and the tidal pool flux of Si_d is less than 3% of the river flux (Buquet et al., 2017). Annual discharge of Mn_d is not available in Arcachon Bay. The uptake of NO_3^- observed in the tidal pool may account for a total NO_3^- removal up to 5000 $kmol.y^{-1}$ that correspond to about 45% of the released NH_4^+. It is worth noting that the presence of *Zostera noltei* within the pool induced an uptake of Si_d that reduced their net release fluxes to the pool water by 30% (Table 1). Tidal pools were not colonized by *Zostera noltei* in 2013, the seagrass only being present at the rim of the pool. Therefore, it is most likely that the seagrass decline observed in the bay since 1989 (Plus et al., 2010) has caused an additional input of Si_d from the tidal pools to the bay waters during the last decades.

Conclusion

This study describes the coupling between water and sediment biogeochemical dynamic in mud flat tidal pools of the Arcachon Bay. Tidal pools are dynamic natural ecosystems where the light irradiance and temperature variations are largely amplified due to the reduced size of the water body, while the effect of evaporation can be neglected. We show that the diagenetic processes are transient in response to tidal and diurnal changes of the physicochemical characteristics in the overlying water. Benthic biogeochemistry is primarily governed by the rapid (minutes time-scale) O_2 variations in surface sediment due to microphytobenthos activity and superficial porewater flushing. Diagenetic processes implying highly sensitive redox species such as H_2S and Mn responded rapidly to these O_2 fluctuations with however a smoother temporal trend attributed to the delay for electron transfer within the chain of redox reactions and chemical transport in sediment. Nutrient (NO_3^-, NH_4^+, PO_4^{3-}) recycling at the sediment water interface did not appear to be closely related to the rapid O_2 dynamic, but likely to longer time-scale cycle associated to the variation in organic matter oxidation processes. The dynamic of Si was mainly driven by the dissolution of biogenic silica, which was directly controlled by temperature. Si releases from the sediment appeared to be lowered in vegetated pools

because of its uptake by *Zostera noltei*. This study showed that tidal pools are easily accessible natural incubators that allow us to apprehend at *in situ* conditions transient biogeochemical processes that occur at the sediment water interface. Tidal pool may also contribute significantly to tidal bay budget of nutrient. Therefore, an all-inclusive budget of nutrient in the Arcachon Bay should take into account benthic fluxes in tidal pools ecosystems.

REFERENCES

Anderson, J.M., Gorley, R.N., Clarke, K.R., 2008. PERMANOVA+ for PRIMER: guide to software and statistical methods. PRIMER-E. Plymouth.

Anschutz, P., Zhong, S., Sundby, B., Mucci, A., & Gobeil, C. (1998). Burial efficiency of phosphorus and the geochemistry of iron in continental margin sediments. *Limnology and Oceanography*, *43*(1), 53–64.

Anschutz, P., Sundby, B., Lefrançois, L., Luther Iii, G. W., & Mucci, A. (2000). Interactions between metal oxides and species of nitrogen and iodine in bioturbated marine sediments. *Geochimica et Cosmochimica Acta*, *64*(16), 2751–2763.

Billerbeck, M., Werner, U., Polerecky, L., Walpersdorf, E., deBeer, D., & Huettel, M. (2006). Surficial and deep pore water circulation governs spatial and temporal scales of nutrient recycling in intertidal sand flat sediment. *Marine Ecology Progress Series*, *326*, 61–76. http://doi.org/10.3354/meps326061

Böttcher, M. E., Hespenheide, B., Llobet-Brossa, E., Beardsley, C., Larsen, O., Schramm, A., … Amann, R. (2000). The biogeochemistry, stable isotope geochemistry, and microbial community structure of a temperate intertidal mudflat: an integrated study. *Continental Shelf Research*, *20*(12–13), 1749–1769. http://doi.org/http://dx.doi.org/10.1016/S0278-4343(00)00046-7

Boudreau, B. P. (1997). *Diagenetic models and their implementation: modelling transport and reactions in aquatic sediments*. (Springer-Verlag, Ed.). Berlin.

Buquet, D., Anschutz, P., Charbonnier, C., Rapin, A., Sinays, R., Canredon, A., … Poirier, D. (2017). Nutrient sequestration in Aquitaine lakes (SW France) limits nutrient flux to the coastal zone. *Journal of Sea Research*, *In Press*.

Burdige, D. J. (2007). Preservation of Organic Matter in Marine Sediments: Controls, Mechanisms, and an Imbalance in Sediment Organic Carbon Budgets? *ChemInform*, *38*(20). http://doi.org/10.1002/chin.200720266

Canton, M., Anschutz, P., Coynel, A., Polsenaere, P., Auby, I., & Poirier, D. (2012). Nutrient export to an Eastern Atlantic coastal zone: first modeling and nitrogen mass balance. *Biogeochemistry*, *107*(1), 361–377.

Charbonnier, C., Anschutz, P., Deflandre, B., Bujan, S., & Lecroart, P. (2016). Measuring pore water properties of exposed beaches using buried probes. *Estuarine, Coastal and Shelf Sciences*, *179*, 66–78.

Clavier, J., Chauvaud, L., Carlier, A., Amice, E., Van der Geest, M., Labrosse, P., … Hily, C. (2011). Aerial and underwater carbon metabolism of a Zostera noltii seagrass bed in the Banc d'Arguin, Mauritania. *Aquatic Botany*, *95*(1), 24–30. http://doi.org/http://dx.doi.org/10.1016/j.aquabot.2011.03.005

Consalvey, M., Paterson, D. M., & Underwood, G. J. C. (2004). The ups and downs of life in a benthic biofilm: migration of benthic diatoms. *Diatom Research*, *19*(2), 181–202. http://doi.org/10.1080/0269249X.2004.9705870

Dalsgaard, T. (2003). Benthic primary production and nutrient cycling in sediments with benthic microalgae and transient accumulation of macroalgae. *Limnology and Oceanography*, *48*(6), 2138–2150.

Daniel, M. J., & Boyden, C. R. (1975). Diurnal variations in physicochemical conditions within intertidal rock pools. *Field Studies Council*, *4*, 161–176.

de Beer, D., Wenzhöfer, F., Ferdelman, T. G., Boeme, S. E., Huettel, M., van Beusekom, J., … Dubilier, N. (2005). Transport and mineralization rates in North Sea sandy intertidal sediments, Sylt-Rømø Basin, Wadden Sea. *Limnology and Oceanography*, *50*(1), 113–127.

Deborde, J., Abril, G., Mouret, A., Jézéquel, D., Thouzeau, G., Clavier, J., … Anschutz, P. (2008). Effects of seasonal dynamics in a Zostera noltii meadow on phosphorus and iron cycles in a tidal mudflat (Arcachon Bay, France). *Marine Ecology Progress Series*, *355*, 59–71. http://doi.org/10.3354/meps07254

Deborde, J., Anschutz, P., Auby, I., Gle, C., Commarieu, M.-V., Maurer, D., … Abril, G. (2008). Role of tidal pumping on nutrient cycling in a temperate lagoon (Arcachon Bay, France). *Marine Chemistry*, *109*, 98–114.

Deflandre, B., & Duchêne, J.-C. (2010). PRO2FLUX - A software program for profile quantification and diffusive O2 flux calculations. *Environmental Modelling & Software*, *25*(9), 1059–1061.

Deflandre, B., Mucci, A., Gagné, J.-P., Guignard, C., & Sundby, B. (2002). Early diagenetic processes in coastal marine sediments disturbed by a catastrophic sedimentation event. *Geochimica et Cosmochimica Acta*, *66*, 2547–2558.

Delgard, M. L., Deflandre, B., Metzger, E., Nuzzio, D., Capo, S., Mouret, A., & Anschutz, P. (2012). In situ study of short-term variations of redox species chemistry in intertidal permeable sediments of the Arcachon lagoon. *Hydrobiologia*, *699*(1), 69–84. http://doi.org/10.1007/s10750-012-1154-5

Delgard, M. L., Deflandre, B., Bernard, G., Richard, M., Kochoni, E., Charbonnier, C., … Anschutz, P. (2016). Benthic oxygen exchange over a heterogeneous Zostera noltei meadow in a temperate coastal ecosystem. *Marine Ecology Progress Series*, *543*, 55–71.

Delgard, M. L., Deflandre, B., Kochoni, E., Avaro, J., Cesbron, F., Bichon, S., … Anschutz, P. (2016). Biogeochemistry of dissolved inorganic carbon and nutrients in seagrass (Zostera noltei) sediments at high and low biomass. *Estuarine, Coastal and Shelf Science*, *179*, 12–22.

Delgard, M.-L., Deflandre, B., Deborde, J., Richard, M., Charbonnier, C., & Anschutz, P. (2013). Changes in Nutrient Biogeochemistry in Response to the Regression of Zostera noltii Meadows in the Arcachon Bay (France). *Aquatic Geochemistry*, *19*(3), 241–259. http://doi.org/10.1007/s10498-013-9192-9

Denis, L., Gevaert, F., & Spilmont, N. (2012). Microphytobenthic production estimated by in situ oxygen microprofiling: short-term dynamics and carbon budget implications. *Journal of Soils and Sediments*, *12*(10), 1517–1529. http://doi.org/10.1007/s11368-012-0588-8

Feuillet-Girard, M., Gouleau, D., Blanchard, G., & Joassard, L. (1997). Nutrient fluxes on an intertidal mudflat in Marennes-Oléron Bay, and influence of the emersion period. *Aquatic Living Resources*, *10*(1), 49–58.

Ganthy, F., Sottolichio, A., & Verney, R. (2013). Seasonal modification of tidal flat sediment dynamics by seagrass meadows of Zostera noltii (Bassin d'Arcachon, France). *Journal of Marine Systems*, 109–110.

Glé, C., Del Amo, Y., Sautour, B., Laborde, P., & Chardy, P. (2008). Variability of nutrients and phytoplankton primary production in a shallow macrotidal coastal ecosystem (Arcachon Bay, France). *Estuarine, Coastal and Shelf Science*, *76*(3), 642–656. http://doi.org/10.1016/j.ecss.2007.07.043

Glud, R. N. (2008). Oxygen dynamics of marine sediments. *Marine Biology Research*, *4*(4), 243–289. http://doi.org/10.1080/17451000801888726

Gunnarsson, I., & Arnorsson, S. (2000). Amorphous silica solubility and the thermodynamic properties of H4SiO4 in the range of 0° to 350°C at Psat. *Geochimica et Cosmochimica Acta*, *64*(13), 2295–2307.

Hall, P. O. J., & Aller, R. C. (1992). Rapid, small-volume, flow injection analysis for ∑CO2 and NH4+ in marine and freshwaters. *Limnology and Oceanography*, *37*, 1113–1119.

Hansen, H. P., & Koroleff, F. (2007). Determination of nutrients. In *Methods of Seawater Analysis* (pp. 159–228). Wiley-VCH Verlag GmbH. http://doi.org/10.1002/9783527613984.ch10

Herman, P. M. J., Hemminga, M. A., Nienhuis, P. H., Verschuure, J. M., & Wessel, E. G. J. (1996). Wax and wane of eelgrass Zostera marina and water column silicon levels. *Marine Ecology Progress Series*, *144*, 303–307. http://doi.org/10.3354/meps144303

Huettel, M., & Webster, I. T. (2001). Porewater flow in permeable sediments. In B. P. Boudreau & B. B. Jørgensen (Eds.), *The benthic boundary layer* (pp. 144–179). Oxford Univ. Press.

Jansen, S., Walpersdorf, E., Werner, U., Billerbeck, M., Böttcher, M. E., & Beer, D. (2009). Functioning of intertidal flats inferred from temporal and spatial dynamics of O2, H2S and pH in their surface sediment. *Ocean Dynamics*, *59*(2), 317–332. http://doi.org/10.1007/s10236-009-0179-4

Jensen, S. L., & Muller-Parker, G. (1994). Inorganic nutrient fluxes in anemone-dominated tide pools. *Pacific Science*, *48*(1), 32–43.

Jørgensen, B. B. (1982). Mineralization of organic matter in the sea bed - the role of sulphate reduction. *Nature*, *296*(5858)), 643–645.

Koroleff, F. (1976). Determination of NH4-N. In K. Grasshoff (Ed.), *Methods of Seawater Analysis* (pp. 127–133). Verlag Chemie.

Kristensen, E. (2000). Organic matter diagenesis at the oxic/anoxic interface in coastal marine sediments, with emphasis on the role of burrowing animals. *Hydrobiologia*, *426*, 1–24.

Kristiansen, K. D., Kristensen, E., & Jensen, E. M. H. (2002). The Influence of Water Column Hypoxia on the Behaviour of Manganese and Iron in Sandy Coastal Marine Sediment. *Estuarine, Coastal and Shelf Science*, *55*(4), 645–654.

Lillebø, A. I., Neto, J. M., Flindt, M. R., Marques, J. C., & Pardal, M. A. (2004). Phosphorous dynamics in a temperate intertidal estuary. *Estuarine, Coastal and Shelf Science*, *61*(1), 101–109. http://doi.org/http://dx.doi.org/10.1016/j.ecss.2004.04.007

Luther, G. W., Sundby, B., Lewis, B. L., Brendel, P. J., & Silverberg, N. (1997). Interactions of manganese with nitrogen cycle: Alternative pathways to dinitrogen. *Geochimica et Cosmochimica Acta*, *61*, 4043–4052.

Malkin, S. Y., & Meysman, F. J. (2015). Rapid redox signal transmission by "Cable Bacteria" beneath a photosynthetic biofilm. *Applied and Environmental Microbiology*, *81*, 948–956.

Marbà, N., Holmer, M., Gacia, E., & Barron, C. (2006). Seagrass Beds and Coastal Biogeochemistry. In *SEAGRASSES: BIOLOGY, ECOLOGY AND CONSERVATION* (pp. 135–157). Springer Netherlands. http://doi.org/10.1007/978-1-4020-2983-7_6

Migné, A., Spilmont, N., Boucher, G., Denis, L., Hubas, C., Janquin, M.A., Rauch, M., Davoult, D., 2009. Annual budget of benthic production in Mont Saint-Michel Bay considering cloudiness, microphytobenthos migration, and variability of respiration rates with tidal conditions. Cont. Shelf Res. 29, 2280–2285. http://dx.doi.org/10.1016/j.csr.2009.09.004.

Morris, S., & Taylor, A. C. (1983). Diurnal and seasonal variation in physico-chemical conditions within intertidal rock pools. *Estuarine, Coastal and Shelf Science*, *17*(3), 339–355. http://doi.org/http://dx.doi.org/10.1016/0272-7714(83)90026-4

Murphy, J., & Riley, J. P. (1962). A modified single solution method for the determination of phosphate in natural waters. *Analytica Chimica Acta*, *27*, 31–36.

Murray, L. G., Mudge, S. M., Newton, A., & Icely, J. D. (2006). The effect of benthic sediments on dissolved nutrient concentrations and fluxes. *Biogeochemistry*, *81*(2), 159–178. http://doi.org/10.1007/s10533-006-9034-6

Nielsen, L. P., & Risgaard-Petersen, N. (2015). Rethinking Sediment Biogeochemistry After the Discovery of Electric Currents. *Annual Review of Marine Science*, *7*(1), 425–442. http://doi.org/10.1146/annurev-marine-010814-015708

Pakhomova, S. V, Hall, P. O. J., Kononets, M. Y., Rozanov, A. G., Tengberg, A., & Vershinin, A. V. (2007). Fluxes of iron and manganese across the sediment-water interface under various redox conditions. *Marine Chemistry*, *107*(3), 319–331.

Plus, M., Dalloyau, S., Trut, G., Auby, I., Montaudouin, X., Emery, E., … Viala, C. (2010). Long-term evolution (1988-2008) of Zostera spp. meadows in Arcachon Bay (Bay of Biscay). *Estuarine, Coastal and Shelf Science*, *87*, 357–36.

Plus, M., Dumas, F., Sanisière, J.-Y., & Maurer, D. (2009). Hydrodynamic charaterisation of the Arcachon Bay, using model-derived descriptors. *Continental Shelf Research*, *29*(8), 1008–1013.

Precht, E., Franke, U., Polerecky, L., & Huettel, M. (2004). Oxygen dynamics in permeable sediments with wave-driven pore water exchange. *Limnology and Oceanography*, *49*, 693–705.

Querné, J., Ragueneau, O., & Poupart, N. (2012). In situ biogenic silica variations in the invasive salt marsh plant, Spartina alterniflora: a possible link with environmental stress. *Plant Soil*, *352*, 157–171.

Raiswell, R., & Canfield, D. E. (2012). The Iron Biogeochemical Cycle Past and Present. *Geochemical Perspectives*, *1*(1), 1–220.

Rigaud, S., Radakovitch, O., Couture, R.-M., Deflandre, B., Cossa, D., Garnier, C., & Garnier, J.-M. (2013). Mobility and fluxes of trace elements and nutrients at the sediment-water interface of a lagoon under contrasting water column oxygenation conditions. *Applied Geochemistry*, *31*, 35–51. http://doi.org/10.1016/j.apgeochem.2012.12.003

Romero, J., Lee, K.-S., Pérez, M., Mateo, M., & Alcoverro, T. (2006). Nutrient Dynamics in Seagrass Ecosystems. In *Seagrasses: Biology, ecology and conservation* (pp. 227–254). Springer Netherlands. http://doi.org/10.1007/978-1-4020-2983-7_9

Schoelynck, J., Bal, K., Backx, H., Okruszko, T., Meire, P., & Struyf, E. (2010). Silica uptake in aquatic and wetland macrophytes: a strategic choice between silica, lignin and cellulose? *New Phytologist*, *186*(2), 385–391. http://doi.org/10.1111/j.1469-8137.2009.03176.x

Slomp, C. P. (2011). Phosphorus Cycling in the Estuarine and Coastal Zones: Sources, Sinks, and Transformations. In E. Wolanski & D. McLusky (Eds.), *Treatise on Estuarine and Coastal Science* (pp. 201–229). Waltham Academic Press.

Smith, K. J., & Able, K. W. (1994). Salt-marsh tide pools as winter refuges for the mummichog, fundulus heteroclitus, in new jersey. *Estuaries*, *17*(1), 226–234.

Soetaert, K., Middelburg, J. J., Herman, P. M. J., & Buis, K. (2000). On the coupling of benthic and pelagic biogeochemical models. *Earth-Science Reviews*, *51*(1–4), 173–201. http://doi.org/http://dx.doi.org/10.1016/S0012-8252(00)00004-0

Sørensen, J., & Jørgensen, B. B. (1987). Early diagenesis in sediments from Danish coastal waters: Microbial activity and Mn-Fe-S geo- chemistry. *Geochimica et Cosmochimica Acta*, *51*, 1583–1590.

Stookey, L. L. (1970). Ferrozine - a new spectrophotometric reagent for iron. *Analytical Chemistry*, *42*(7), 779–781. http://doi.org/10.1021/ac60289a016

Sundby, B., Anderson, L. G., Hall, P. O. J., Iverfeldt, ≈ke, van der Loeff, M. M. R., & Westerlund, S. F. G. (1986). The effect of oxygen on release and uptake of cobalt, manganese, iron and phosphate at the sediment-water interface. *Geochimica et Cosmochimica Acta*, *50*(6), 1281–1288.

Taillefert, M., Neuhuber, S., & Bristow, G. (2007). The effect of tidal forcing on biogeochemical processes in intertidal salt marsh sediments. *Geochemical Transactions*, *8*(1), 1–15. http://doi.org/10.1186/1467-4866-8-6

Takeuchi, S., & Tamaki, A. (2014). Assessment of benthic disturbance associated with stingray foraging for ghost shrimp by aerial survey over an intertidal sandflat. *Continental Shelf Research*, *84*, 139–157. http://doi.org/10.1016/j.csr.2014.05.007

Thamdrup, B., Hansen, J. W., & Jørgensen, B. B. (1998). Temperature dependence of aerobic respiration in a coastal sediment. *FEMS Microbiology Ecology*, *25*, 189–200.

Truesdale, V. W., & Smith, C. J. (1976). The automatic determination of silicate dissolved in natural fresh water by means of procedures involving the use of either α- or β- molybdosilicic acid. *The Analyst*, 19–31.

van der Laan, B. B. P. A., & Wolff, W. J. (2006). Circular pools in the seagrass beds of the Banc d'Arguin, Mauritania, and their possible origin. *Aquatic Botany*, *84*(2), 93–100. http://doi.org/http://dx.doi.org/10.1016/j.aquabot.2005.07.009

Werner, U., Billerbeck, M., Polerecky, L., Franke, U., Huettel, M., van Beusekom, J. E. E., & de Beer, D. (2006). Spatial and temporal patterns of mineralization rates and oxygen distribution in a permeable intertidal sand flat (Sylt, Germany). *Limnology and Oceanography*, *51*(6), 2549–2563.

Wilson, C. A., Hughes, Z. J., FitzGerald, D. M., Hopkinson, C. S., Valentine, V., & Kolker, A. S. (2014). Saltmarsh pool and tidal creek morphodynamics: Dynamic equilibrium of northern latitude saltmarshes? *Geomorphology*, *213*, 99–115.

TABLES AND TABLES CAPTIONS

Table 1: General information and total fluxes of nutrients (NO_3^-, NH_4^+, PO_4^{3-} and Si_d) and dissolved Mn (Mn_d) in intertidal pools studied the July 1st 2010 (two vegetated and two unvegetated pools), 27-28 August (same pool, day and night) and 8-10 October (same pool, 3 consecutive days). Fluxes were calculated from concentrations change in the isolated pool water. No flux of dissolved Fe was reported as Fe concentration was always below the detection limit. The uncertainties associated to fluxes correspond to the standard error associated to the slope of the linear regression and n is the number of data point used for the linear regression. Fluxes associated with the same letter correspond to those for which no significant (adjusted p>0.05) differences in the slopes were detected using pairwise slope homogeneity test (p values adjusted using Holm-Bonferroni method)

Date	Pool number	Substrate	Pool diameter (m)	Pool depth (cm)	Condition	T (°C)	Salinity	n	NO$_3^-$	NH$_4^+$	PO$_4^{3-}$	Si$_d$	Mn$_d$
									Fluxes (µmol.m^{-2}.h^{-1})				
July 2010	1	Zostera sp.	3.6	2.5	Day	38.0 ± 2.0	32.2 ± 0.7	12	<lq	<lq	0.53±0.14[a]	426±63[ab]	n.d.
	3	Zostera sp.	1.4	1.0	Day	38.1 ± 0.8	n.d.	8	<lq	<lq	0.67±0.17[ab]	339±13[a]	n.d.
	2	Unvegetated	2.5	2.5	Day	38.0 ± 2.0	n.d.	8	<lq	<lq	n.s.	605±105[a]	n.d.
	4	Unvegetated	3.6	10	Day	38.0 ± 2.0	n.d.	8	<lq	<lq	n.s.	620±112[a]	n.d.
August 2013	5	Unvegetated	4.0	12	Day	27.0 ± 1.0	33.1 ± 0.2	8	n.s.	119±32[a]	n.s.	182±25[b]	4.1±1.4[a]
					Night	19.3 ± 0.5	32.74 ± 0.04	8	-15±2[a]	81±29[ab]	2.8±0.7[bc]	49±6[d]	41±4[b]
October 2013	6	Unvegetated	4.5	12	Day	21.7 ± 0.3	31.6 ± 0.2	12	-33±5[a]	33±3[b]	4.5±0.3[c]	68±5[cd]	n.s.
					Day	22.9 ± 0.6	32.5 ± 0.2	13	n.s.	52±9[ab]	3.4±0.7[abc]	83±5[c]	4.6±2.3[a]
					Day	20 ± 1	33.2 ± 0.3	9	-53±15[a]	n.s.	3.1±0.8[abc]	61±2[cd]	6.8±2.1[a]

<lq: concentrations lower than the limit of quantification / n.d.: not determined / n.s.: not significant (p<0.05) slope
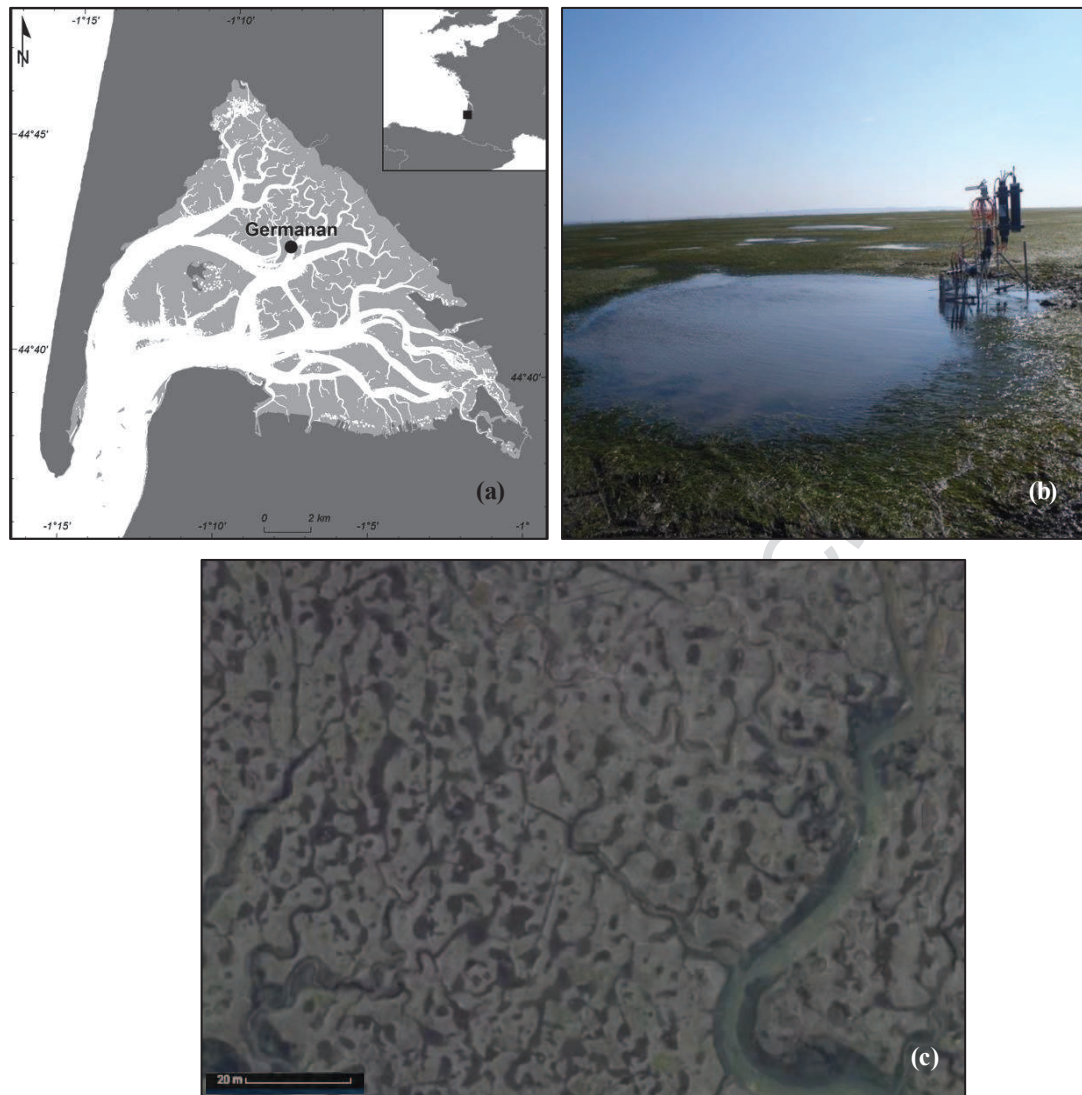
detected.

FIGURES

Figure 1: (a) Map of the Arcachon Bay (France) showing the location of the sampling site Germanan. (b) Photo of an intertidal pool studied in the *Zostera noltei* meadow of Germanan with the MP6 miniprofiler system. (c) Example of an aerial photo of the intertidal flat studied showing the numerous tidal pools (Image @2017 Google).
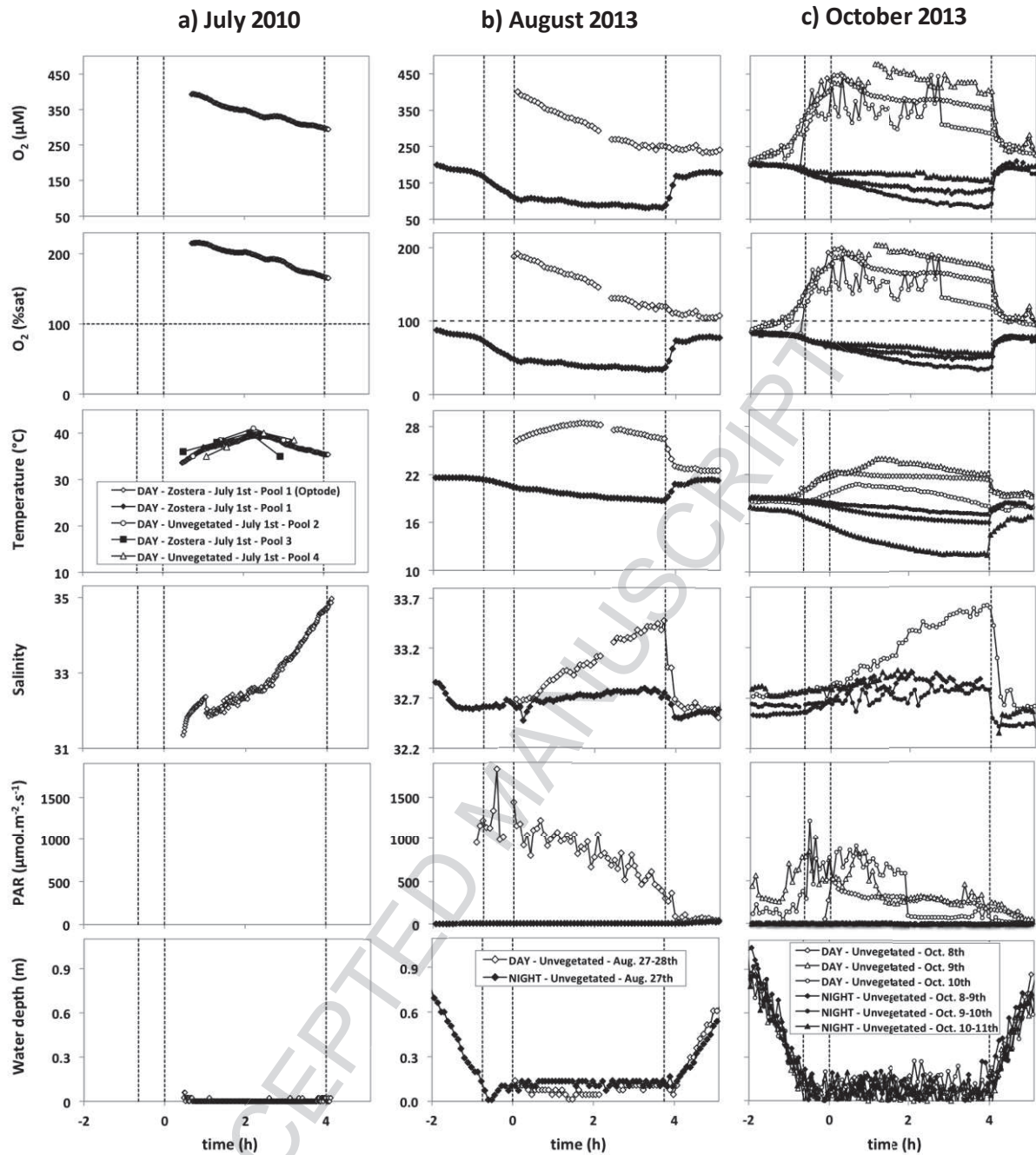
Figure 2: Evolution of O_2 concentrations and physicochemical properties in the intertidal pools studied (a) during daytime in one of the four pools the July 1st 2010, (b) during daytime and the following night the 27-28 August 2013 and (c) during three consecutive days the 8-10 October 2013. Note the different scales for temperature and salinity in July 2010. The three vertical dashed lines indicate the beginning of the pool isolation (left), the time when the water of the intertidal flat ceased to flow through the pool (set at 0 h), and the time of pool inundation at flood tide (right).

Figure 3. Evolution of chemical composition of pool water (a) in four pools during daytime the July 1st 2010, (b) in one pool during daytime and the following night the 27-28 August 2013 and (c) in one pool during three consecutive days the 8-10 October 2013. Note the different scales for Si_d and PO_4^{3-} in July 2010. The three vertical dashed lines indicate the beginning of the pool isolation (left), the time when the water of the intertidal flat ceased to flow through the pool (set at 0 h), and the time of pool inundation at flood tide (right). Note that dissolved Fe was always below the detection limit.
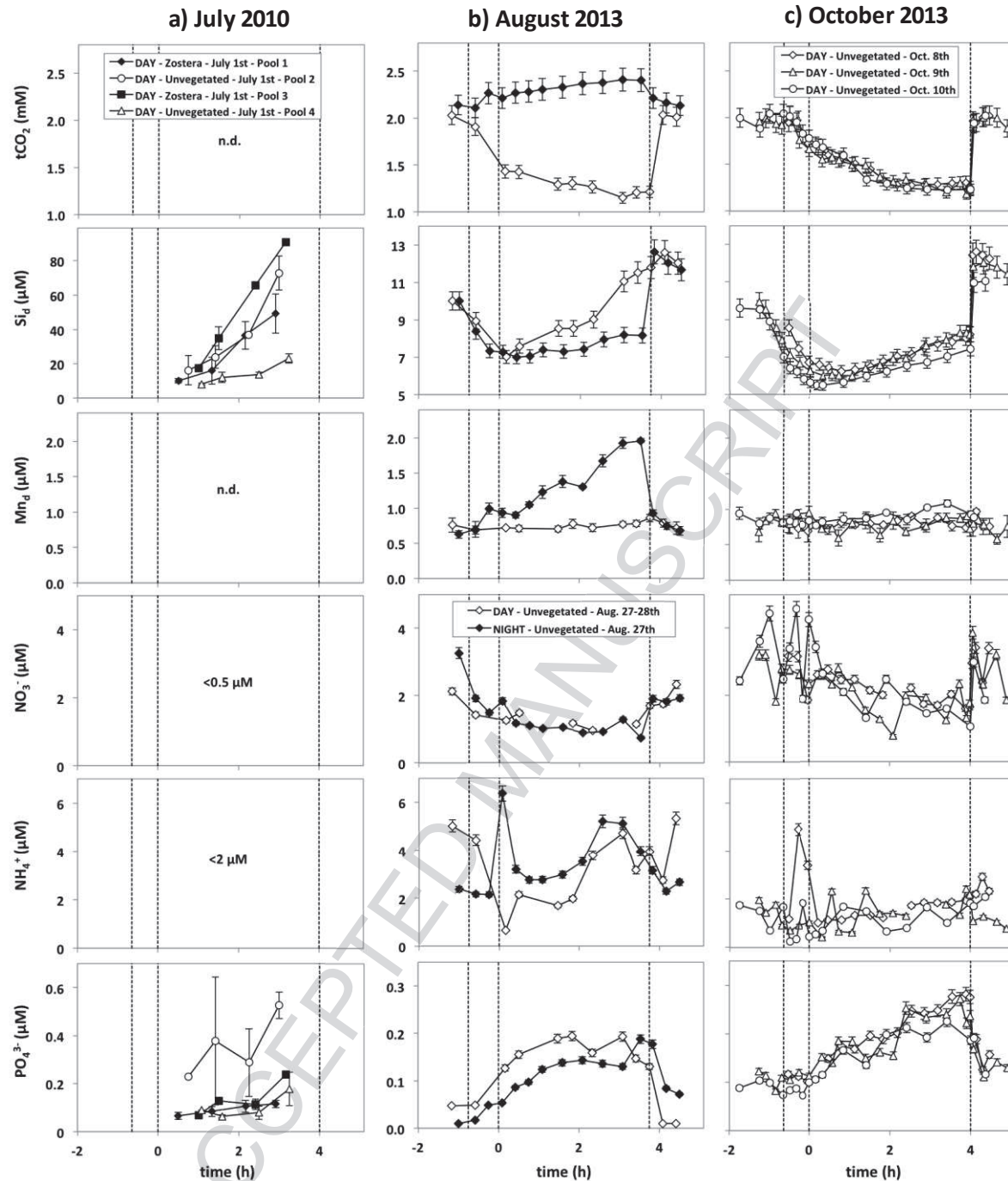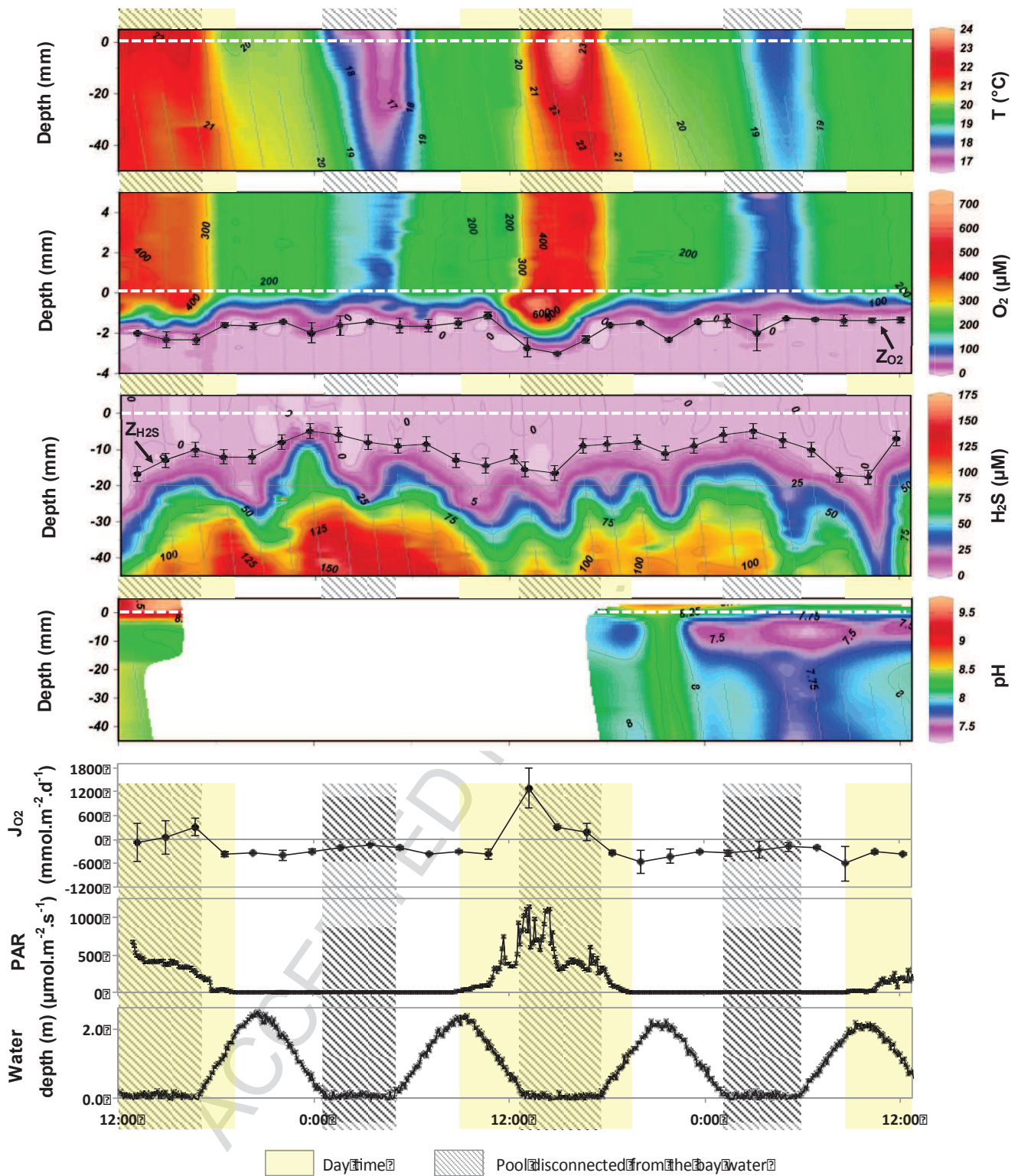
Figure 4: Vertical distribution of temperature, O_2 and H_2S concentrations and pH in pool sediment measured by microsensors for a 48h period the 8-10 October 2013. The 2D mapping was carried out using the DIVA gridding mode of the Ocean Data View software (Schlitzer, 2014). The O_2 penetration depths (Z_{O2}), H_2S apparition depths (Z_{H2S}) and diffusive O_2 fluxes at the sediment-water interface (JO_2) obtained from the depth profiles are also reported. Negative JO_2 values correspond to fluxes from the water to the sediment. Values reported for J_{O2} and Z_{O2} correspond to the average of 3 profiles and the error bars correspond to ± 1 standard deviation. The error bars for H_2S apparition depths correspond to ± 1 mm assumed to be the uncertainty on the interface detection on H_2S profiles. The horizontal white dashed lines correspond to the sediment-water interface. PAR and water depth are

also reported with the periods when the pool was disconnected from the bay water (dashed area) and the daytime period (light shaded areas). The absence of pH values is due to a broken electrode during the profiling sequence.

Figure 5. Evolution of O_2 and H_2S concentrations, pH and temperature in the sediment measured using microsensors for a 24h period the 10-11 October 2013. Temperature and oxygen concentration in the pool water as well as light (PAR) and water depth are also reported.

Figure 6. Si_d fluxes vs. average temperature in the unvegetated intertidal pools. Fluxes were calculated from concentrations change in the pool water at low tide. The error bars associated to fluxes correspond to the uncertainty associated to the slope of the linear regression. The error bars associated to the temperature correspond to the standard deviation around the average during pool disconnection.

APPENDICES

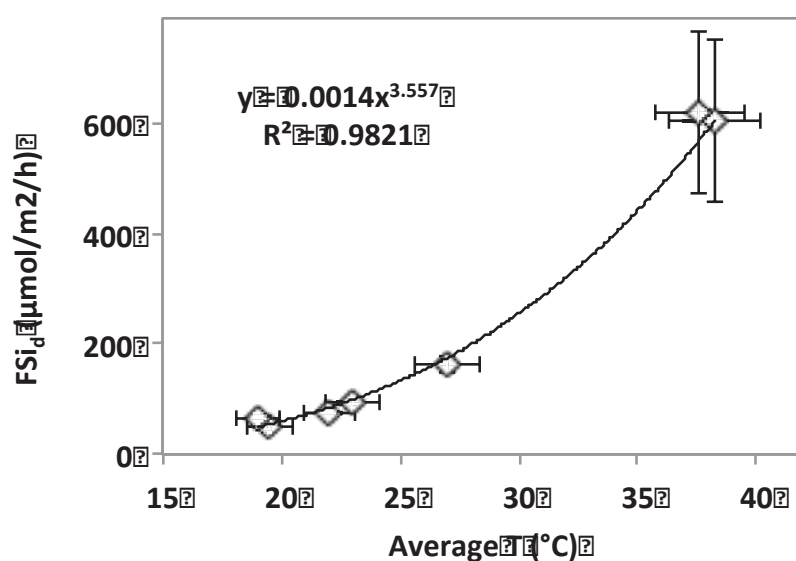Table A1: Distance Based Linear Model results between predictors (Temperature and Photosynthetically Active Radiation, PAR) and the concentration patterns of O_2 and tCO_2 (in a multivariate space defined using Euclidean distance) in the pool water during disconnection from the bay water. Marginal tests show the proportion of variation explained by predictor variables fitted individually. Sequential tests (using a Forward selection and AIC selection criteria) determine the variance explained by predictor variables when fitted sequentially. AIC (Akaike Information Criteria) is the criteria used for model selection, the lower the AIC, the better the model (conversely to R², AIC is not affected by the number of fitted variables). pseudo-F indicate the statistic (using permutations) used to test the significativity of the model selected against the hypothesis of no relationship between the response data cloud and the model chosen (predictors).

Tidal pool campaign	Test	Variable	AIC	Pseudo-F	p value	Prop. of variance explained
August 2013 - Night	Marginal tests	T(°C)		106.8	0.001	94.7%
August 2013 - Day	Marginal tests	T (°C) PAR ($\mu mol.m^{-2}.s^{-1}$)		3.8 31.3	0.104 0.002	43.1% 86.2%
	Sequential tests	PAR ($\mu mol.m^{-2}.s^{-1}$) + T (°C)	-6.1 -11.2	31.3 7.06	0,001 0.021	86.2% 95.0%
October 2013 - Day 1	Marginal tests	T (°C) PAR ($\mu mol.m^{-2}.s^{-1}$)		64.8 14.1	0.001 0.003	87.8% 61.1%
	Sequential tests	T (°C)	-12.6	64.8	0,001	87.8%
October 2013 - Day 2	Marginal tests	T (°C) PAR ($\mu mol.m^{-2}.s^{-1}$)		7.2 4.3	0.017 0.026	47.3% 35.1%
	Sequential tests	T (°C) +PAR ($\mu mol.m^{-2}.s^{-1}$)	3.5 -2.0	7.2 7.8	0.02 0.03	47.3% 75.0%
October 2013 - Day 3	Marginal tests	T (°C) PAR ($\mu mol.m^{-2}.s^{-1}$)		11.7 10.7	0.002 0.006	62.6% 60.3%
	Sequential tests	T (°C) +PAR ($\mu mol.m^{-2}.s^{-1}$)	0.3 -4.5	11.7 6.8	0.001 0.017	62.6% 82.5%

Table A2: Distance Based Linear Model results between predictors variables (abiotic drivers) and the temporal variation of sediment processes. Marginal tests show the proportion of temporal variation explained by predictor variables fitted individually. Sequential tests (using a Forward selection and AIC selection criteria) determine the variance explained by predictor variables when fitted sequentially. AIC (Akaike Information Criteria) is the criteria used for model selection, the lower the AIC, the better the model (conversely to R^2, AIC is not affected by the number of fitted variables). pseudo-F indicate the statistic (using permutations) used to test the significativity of the model selected against the hypothesis of no relationship between the response data cloud and the model chosen (predictors).

Tidal pool campaign	Response variables	Test	Variable	AIC	Pseudo-F	p value	Prop. of variation explained
October 2013 – profiling experiment	Oxygen diffusive fluxes	Marginal tests	Water depth (m) T (°C) PAR ($\mu mol.m^{-2}.s^{-1}$)		10.6 8.2 104.5	0.001 0.012 0.001	29.9% 24.7% 80.7%
		Sequential tests	PAR ($\mu mol.m^{-2}.s^{-1}$) +Water depth (m)	76.5 69.9	104.5 9.0	0.001 0.006	80.7% 86.0%
October 2013 – profiling experiment	Oxygen penetration depth	Marginal tests	Water depth (m) T (°C) PAR ($\mu mol.m^{-2}.s^{-1}$)		4.9 32.2 16.6	0.036 0.001 0.002	16.3% 56.3% 39.9%
		Sequential tests	T (°C) +PAR ($\mu mol.m^{-2}.s^{-1}$)	-59.3 -62.1	32.2 4.6	0.001 0.047	56.3% 63.4%
October 2013 – profiling experiment	H_2S appearance depth	Marginal tests	Water depth (m) T (°C) PAR ($\mu mol.m^{-2}.s^{-1}$) O_2 penetration depth		2.1 7.4 5.7 1.8	0.155 0.006 0.018 0.188	7.8% 22.9% 18.5% 6.7%
		Sequential tests	T (°C) +Water depth (m) +PAR ($\mu mol.m^{-2}.s^{-1}$)	68.6 64.9 61.3	7.4 5.6 5.3	0.012 0.027 0.023	22.9% 37.5% 49.3%
October 2013 – time-series experiment	Oxygen concentration in surface sediment (-0.5, -1.1, -1.7 mm)	Marginal tests	T (°C) Water depth (m) Sediment T (°C) PAR ($\mu mol.m^{-2}.s^{-1}$)		150.5 8.2 103.0 603.5	0.001 0.005 0.001 0.001	35.4% 28.8% 27.2% 68.7%
		Sequential tests	PAR ($\mu mol.m^{-2}.s^{-1}$) +T (°C) +Water depth (m)	2419.4 2385.9 2372.0	603.5 37.4 16.1	0.001 0.001 0.001	68.7% 72.5% 74.0%
October 2013 –time-series experiment	H_2S concentration in sediment (-2.5 cm)	Marginal tests	T (°C) Water depth (m) Sediment T (°C) PAR ($\mu mol.m^{-2}.s^{-1}$)		14.8 1013.4 9.5 28.8	0.003 0.001 0.001 0.001	50.9% 78.7% 33.3% 9.4%
		Sequential tests	Water depth (m)	616.1	1013.4	0.001	78.7%
October 2013 –time-	pH in sediment (-2.5 cm)	Marginal tests	T (°C) Water depth (m)		67.7 15.8	0.001 0.001	19.8% 5.4%

series experiment			Sediment T (°C) PAR ($\mu mol.m^{-2}.s^{-1}$)		96.0 109.3	0.001 0.001	25.9% 28.4%
		Sequential tests	PAR ($\mu mol.m^{-2}.s^{-1}$) +Sediment T (°C) +T (°C) +Water depth (m)	-2380.6 -2419.5 -2477.4 -2479.6	109.3 43.6 65.9 4.1	0.001 0.001 0.001 0.035	28.4% 38.2% 50.3% 51.0%

HIGHLIGHTS

- Tidal pools are natural and very dynamic small-scale ecosystems
- They are suitable to investigate the transient dynamic of benthic biogeochemical processes
- Temperature, light and hydrodynamic are the main driving factors
- O_2, CO_2, sulphide and metals fluctuate at diurnal and tidal timescales
- Tidal pools play a significant role in the biogeochemical functioning of Arcachon Bay